IN 2003, NEXRAIN BECAME ONERAIN INCORPORATED (ONERAIN.COM)

Storm Sizes and Shapes in the Arid Southwest

by

David C. Curtis, Ph.D.
NEXRAIN Corporation
Orangevale, CA 95662

Introduction

A historical database of 2 km x 2 km 15-minute radar-rainfall estimates was used to study the sizes, shapes, orientations, and depth-area characteristics of storms in Clark County, NV. More than 100,000 individual 15-minute storms were evaluated over a four year period. The size, shape, orientation, track, and the three-dimensional characteristics of each storm were cataloged.

Background

Clark County encompasses approximately 7910 square miles of territory typical of the arid southwest. The climate is dry with average annual rainfall at Las Vegas averaging a little over 4 inches per year. Monthly average rainfall ranges from 0.1-0.5 inches. Small scale thunderstorm activity dominates the summer time rainfall pattern with July, August, and September the prime months for flash floods. More widespread rainfall patterms are typical in the winter months of December, January, and February.

Approximately 96% of the population of Clark County lives in the Las Vegas Valley with smaller population centers in Laughlin, Mesquite, and the Moapa Valley. The urbanized portion of the Las Vegas Valley includes about 625 square miles.

The distribution of rain gages in Clark County closely maps the population distribution. The Las Vegas Valley contains 88 of the 121 rain gages in the RFCD network. Ten gages are located in southern Clark County and the remaining 23 gages are in northeast Clark County.

The overall gage density for the county is about one gage in 65 square miles. However, the current density in the more populated portions of the Las Vegas Valley is approximately one gage in seven square miles.

Methodology

Radar provides continuous spatial coverage of rain events and can show the actual sizes, shapes, and tracks of individual storms. Now that an extensive network of radars has been operating for several years, a database of historical radar-rainfall estimates is available for statistical analysis of storm properties. These storm properties can provide useful guidance for a wide range of issues including rain gage network evaluation and the development of design storms.

Historical 15-minute, 2 km x 2 km radar-rainfall estimates from May 1995 to December 1999 were obtained for Clark County and surrounding areas of Nevada, California, Arizona, and southwest Utah. Data for areas outside of Clark County were included to minimize edge effects on statistics near the county borders.

The radar-rainfall estimates were extracted from NEXRAIN's national database of 15-minute, 2 km x 2 km radar-rainfall estimates. These data were originally obtained from WSI Corporation located in Billerica, MA. WSI creates a national mosaic of radar-rainfall estimates every 15-minutes. This mosaic is constructed from data from all National Weather Service and US Department of Defense WSR-88D radars. NWS radars from Las Vegas, NV and Cedar City, UT as well as the DOD radar at Edwards AFB in California cover all or portions of Clark County. Where one or more radars overlap, the highest rainfall value at each pixel is used. Rainfall estimates are derived using reflectivity from the lowest available tilt angles at each radar.

WSI's rainfall estimation procedure uses a dynamic weather condition-based algorithm to convert reflectivity values to rainfall estimates. The WSI procedure uses a variety of weather parameters to sense what type of weather condition exists, then chooses the most appropriate conversion from reflectivity to rainfall rate.

Rain gage data for the region were obtained from the National Weather Service to calibrate the radar-rainfall data set. Daily, hourly, and 15-minute gage data were used to calibrate the radar estimates. Since an insufficient number of 15-minute rain gage records existed over the entire study region to perform a detailed calibration, daily and hourly data were disaggregated to 15-minute time steps using the normalized radar data at each gage location as the distribution function. Calibrations were performed to adjust the radar estimates to match the rain gage estimates, on average, at the monthly level.

A specialized software package called Titan (Dixon, 1993 & 1994) was used to review the 15-minute gage-adjusted radar-rainfall estimates to identify and track contiguous areas of rainfall. Only storm areas with intensities greater than approximately 0.08 iph were considered. For each area of rainfall identified, an ellipse was *fit* to the area and its properties (e.g. area, long and short axis lengths, orientation, peak intensity, direction of motion, and speed, etc.) were recorded. For the purposes of this study, each area of contiguous rainfall is called a *storm*.

Figure 1 shows the daily summary of all the storms identified for May 16, 1995. Each 15-minute storm ellipse is shown with a motion vector. Alternate colors of light and dark green simply distinguish ellipses for successive periods. On this day of light activity, only a few small isolated storms were identified, with only one storm track longer than a period or two.

Figure 2 shows the summary for the next day, May 17, 1995. Storms were more widespread but the storms were still fairly isolated and short lived.

Larger storms more characteristic of a winter event are shown in Figures 3 and 4. Figure 3 shows the storms identified for February 6, 1998. On this day, the leading edge of a storm complex began to enter the region. A small number of larger areas of rain were identified along with a larger number of small storms. Storms for the following day, February 7, 1998, are shown in Figure 4. On this day, the entire county was covered by storms at one time or another. The storm sizes are significantly larger in size as expected in a winter storm event.

In all, 124,234 individual 15-minute storms were identified, tracked, and categorized. The histogram of storm areas is shown in Figure 5. Storm sizes ranged from a minimum of 12 square miles to a maximum of 9,402 square miles with a mean of 103 square miles and a median of 32 square miles. The distribution shown in Figure 5 is heavily skewed toward small storms. Fifty percent of the 124,234 storms analyzed were less than 32 square miles.

Figure 6 shows the frequency distribution of the ellipses fit to the 124, 234 individual 15-minute storms. The vast majority (~89%) of the individual storms had aspect ratios (long axis divided by short axis) between 1:1 and 3:1. (This is a good confirmation of a common engineering design practice of using a storm aspect ratio of 2:1 for design storms.)

Figure 7 shows the distribution of storm orientations. Storm orientation is defined as the angle of the long axis of the storm ellipse from north. The most common storm orientations are in the range of 70-90 degrees from north. However, the overall distribution is fairly flat.

A variety of storm characteristics are shown spatially in Figures 8-22. Figure 8 shows the overall distribution of rainfall during the entire study period. As expected, the areas of higher rainfall are associated with higher elevation mountain peaks in and near Clark County. Lower amounts of rainfall are seen in the valley areas. However, the low rainfall amounts in extreme western Clark County are associated with radar beam blockage by the mountains and due to lack of radar coverage in the northwest corner of the study area during the first two years of the study period.

Also plotted on Figure 8 are mean storm vectors summarizing the relative speed and direction of storm movement over the entire study period. Average storm movement over Clark County is strongly west to east and quite uniformly so over the entire county.

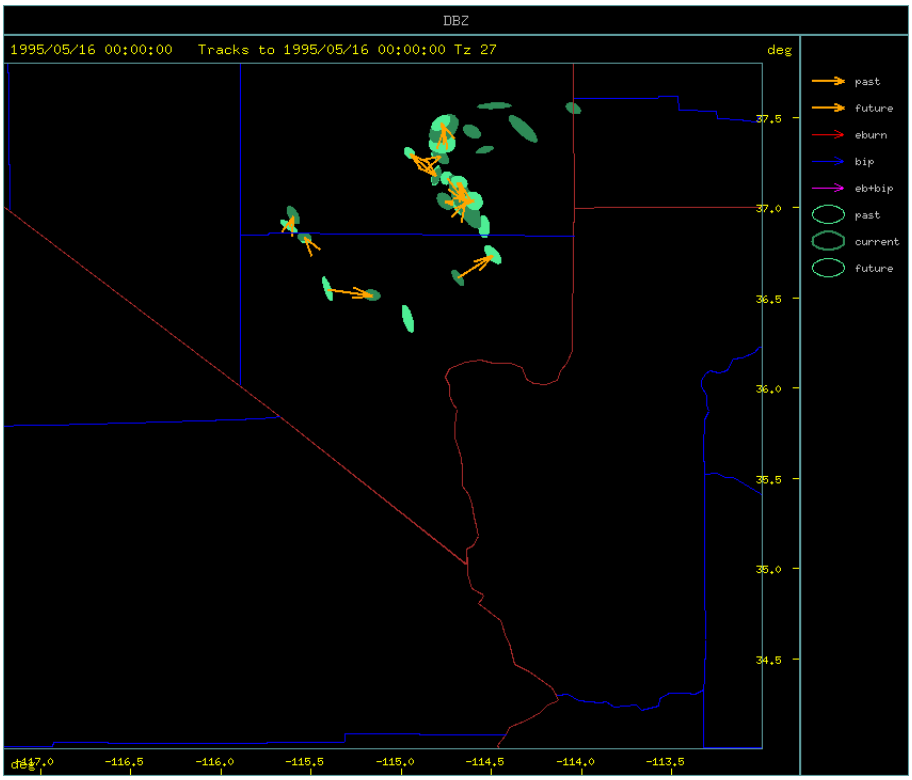

Figure 1: Daily storm ellipse summary for May 16, 1995

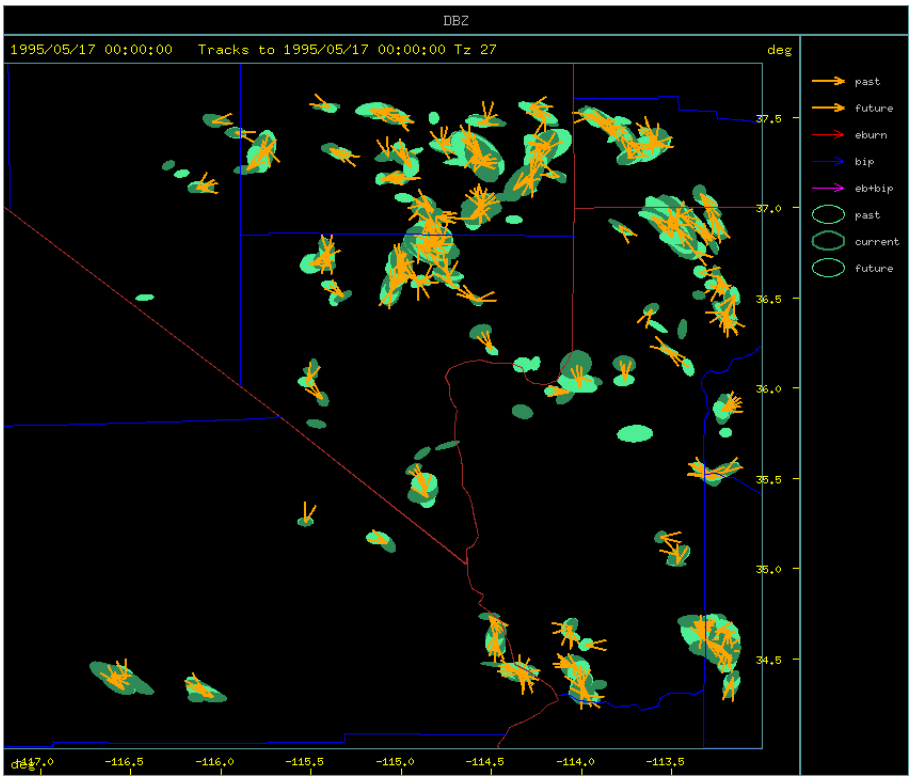

Figure 2: Daily storm ellipse summary for May 17, 1995

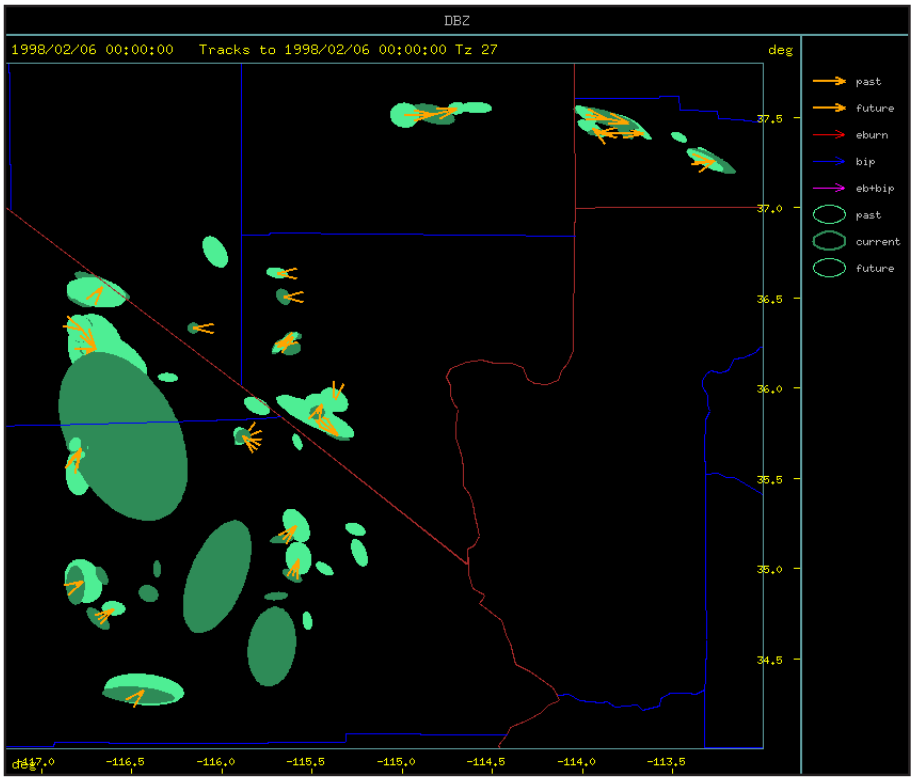

Figure 3: Daily storm ellipse summary for February 6, 1998.

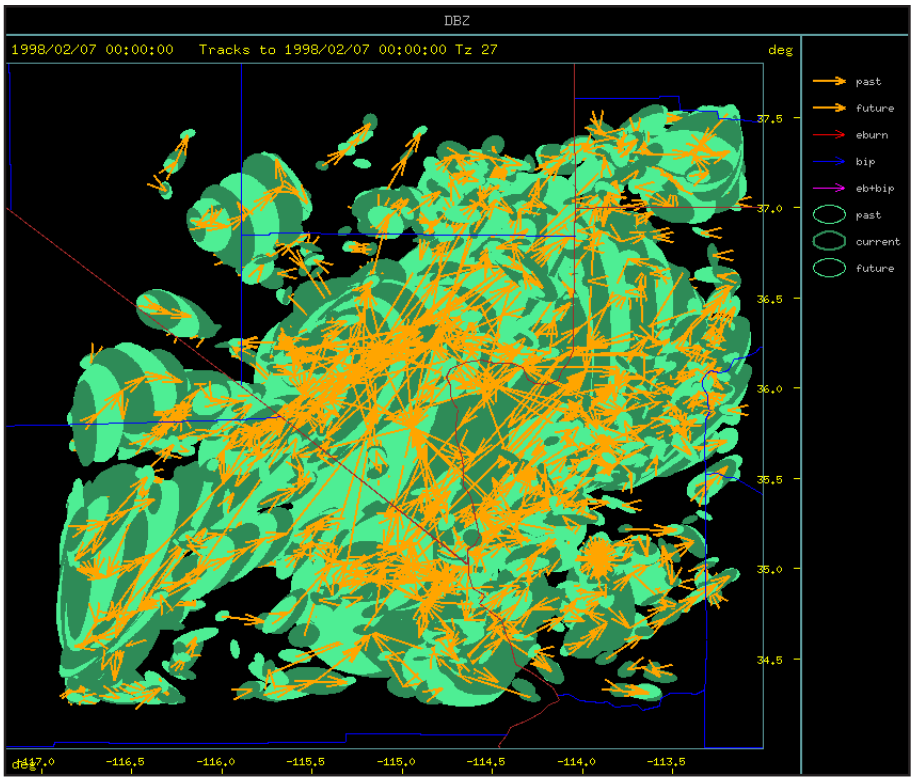

Figure 4: Daily storm ellipse summary for February 7, 1998.

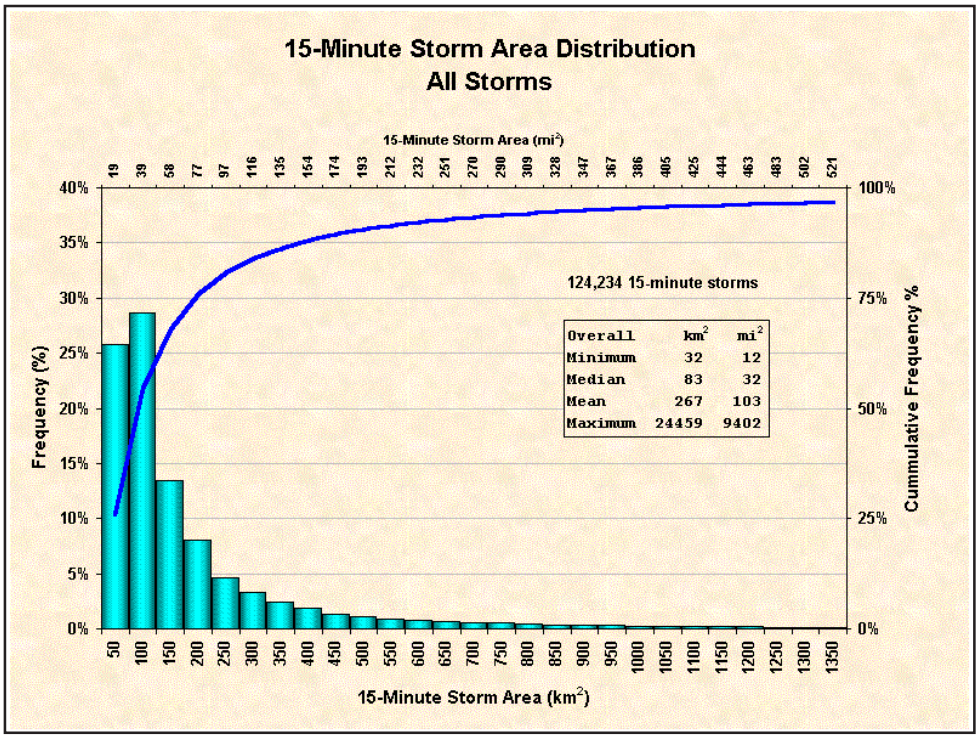

Figure 5: Frequency distribution of storm sizes.

Figure 6: Frequency distribution of storm aspect ratio.

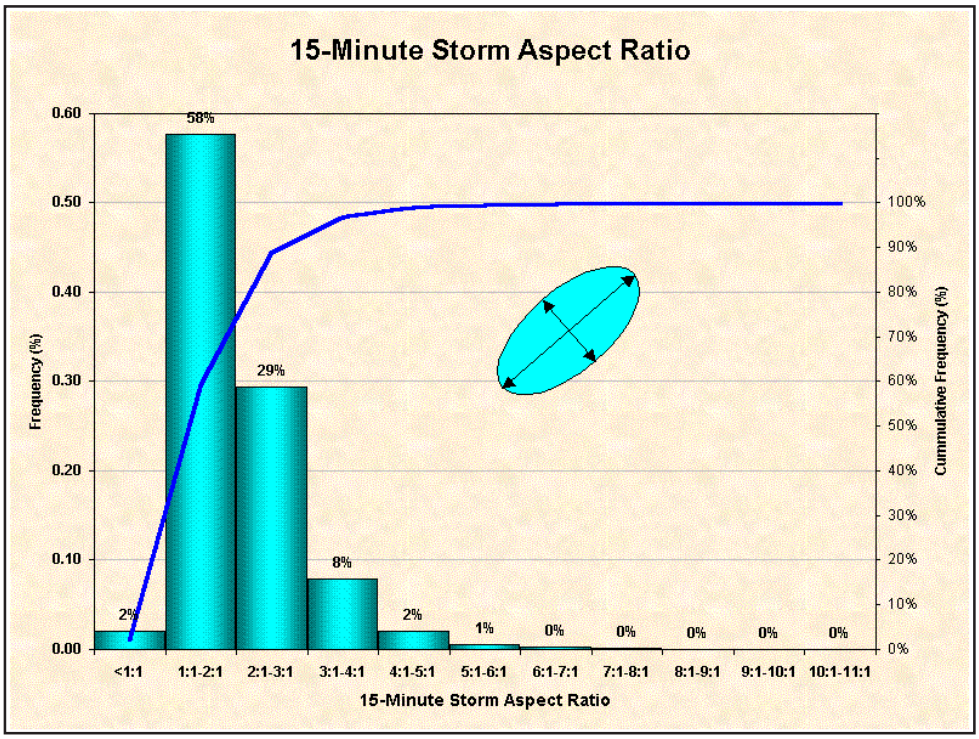

Figure 7: Frequency distribution of storm orientation.

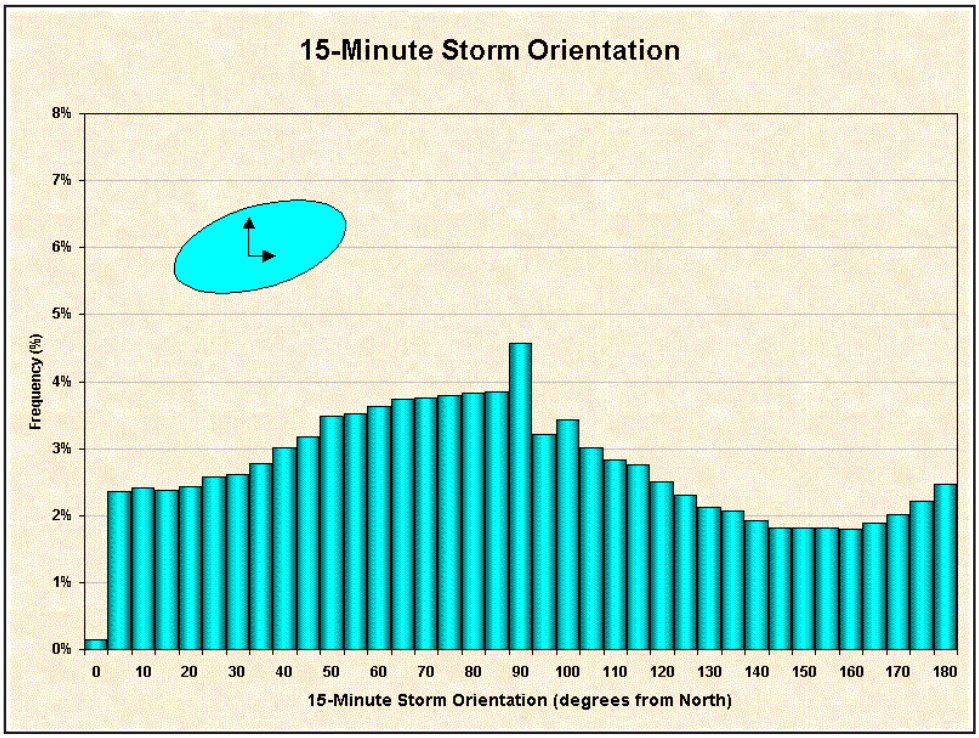

Figure 8: Distribution of accumulated rainfall.

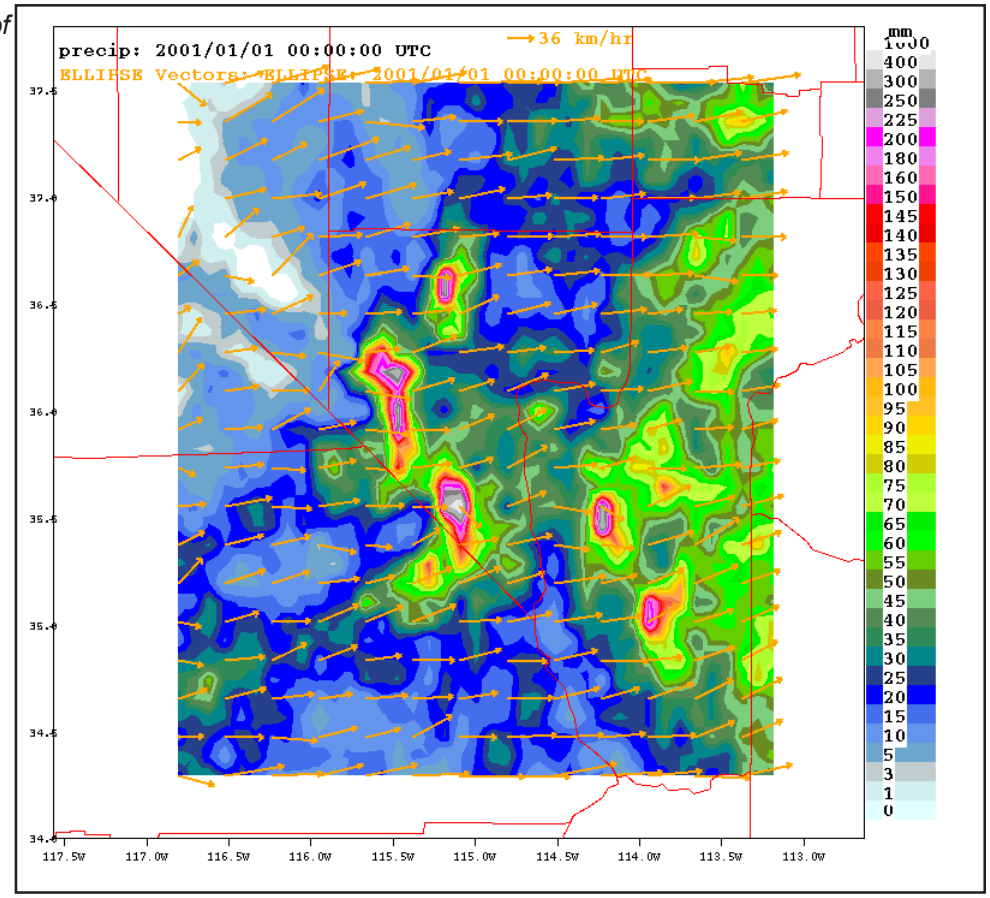

Figure 9: Distribution of mean storm area.

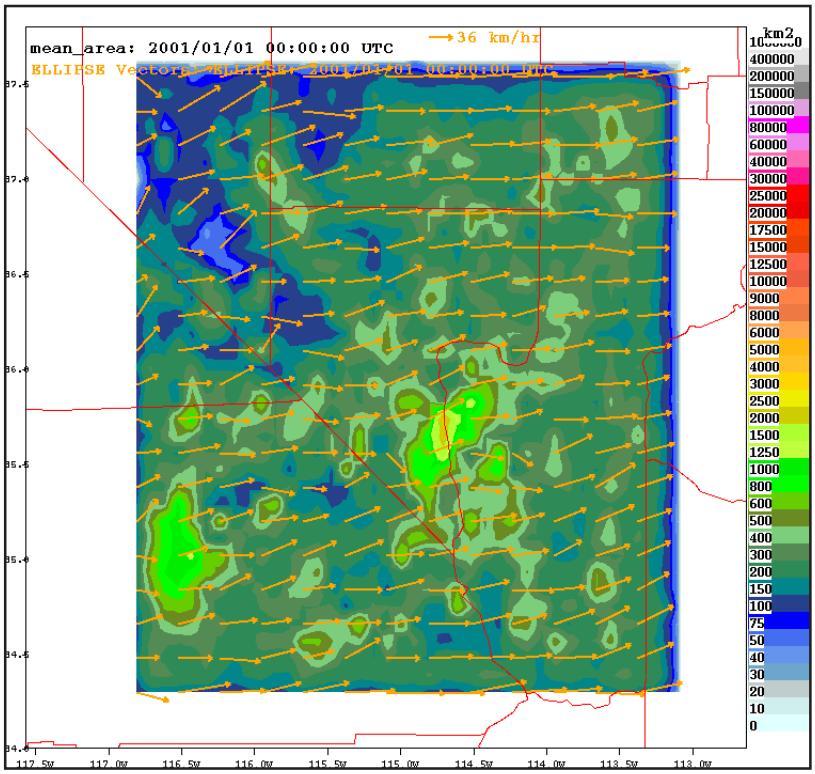

Figure 10: Distribution of storm starts.

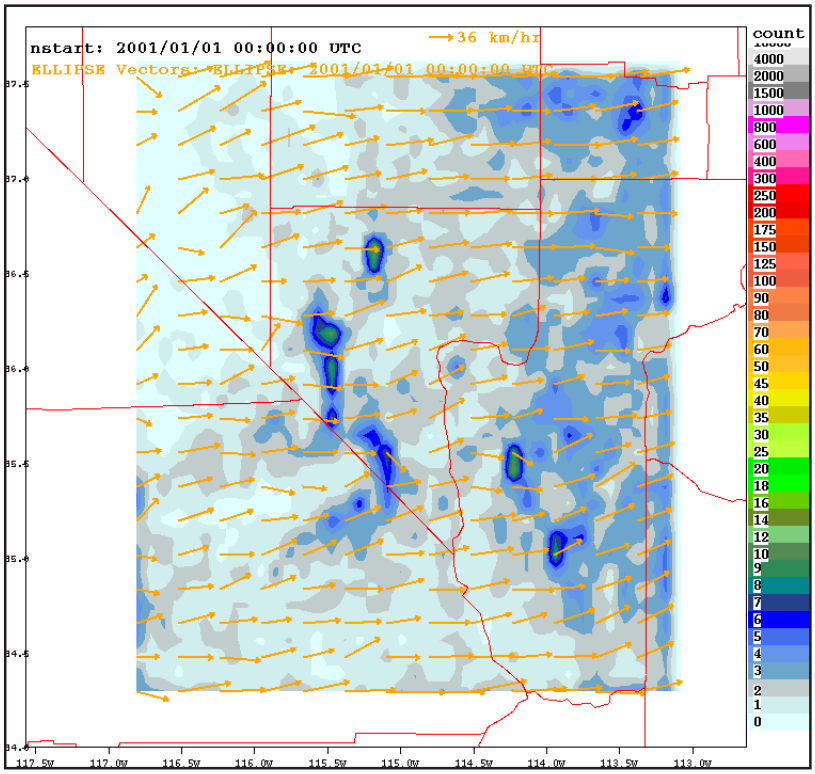

Figure 9 presents the spatial distribution of mean storm area over the county. With the exception of a small area south of Las Vegas, mean storm size is fairly uniform spatially.

Figure 10 presents a measure of storm activity in the region. The number of times a storm started at a given pixel location was recorded throughout the study period and the results are indicated in Figure 10. The regions associated with the highest number of storm starts are the higher elevation regions, indicating a significant orographic influence on the initiation of storm activity in Clark County.

Figures 11-22 show monthly storm properties, including storm activity (the number of times storms were observed at each pixel location) and the monthly storm vectors. Higher amounts of storm activity are again associated with the higher elevation areas. Since there was not an equal number of months for each month during the study period due to missing radar data, it's difficult to draw too many conclusions from these figures.

What seems interesting with Figures 11-22, however, is the monthly storm vectors. The storm vectors appear more chaotic due the smaller numbers of events than the storm vectors of Figure 8 which summarize the entire study period. However, the storm vectors for each month are quite similar. Each month shows a strong west to east component to storm movement. Surprisingly, there is not a pronounced seasonality that might be expected with monsoonal activity. Perhaps the study period was too short to notice a strong seasonal component to storm movement.

Figure 23 shows the depth-area curves for storms over a range of peak rainfall intensities. During the Titan analysis as each elliptical shaped storm was identified, the peak rainfall intensity was recorded along with the area of each intensity contour in the storm from the peak intensity down to approximately 0.08 iph. In addition, the minimum, median, mean, and maximum total storm area for each intensity range was computed (See Table 1).

Table 1: Peak Rainfall Intensity (iph)

	0.29	**0.39**	**0.53**	**0.71**	**0.94**	**1.26**	**1.67**	**2.23**	**2.98**	**3.97**
No. of storms	10167	11989	9257	6768	4827	3269	1666	726	241	36
Min (mi^2)	12	12	12	12	12	12	12	12	12	12
Median (mi^2)	37	45	49	65	79	97	126	160	347	255
Mean (mi^2)	93	109	124	160	210	272	461	690	1700	712
Max (mi^2)	5102	5020	3831	3924	6618	7038	8134	9444	9050	4558

The curves in Figure 23 represent the idealized cross-sections of the elliptical shapes fit to the storms at each peak rainfall intensity. The amount of storm area for each rainfall intensity contour was computed as a percentage of total storm area. Storms of all sizes for a given peak intensity were used to compute average contour areas as percentages of total storm area. The depth-area curves shown in Figure 23 were then constructed using the contour percentages and the median storm size for each peak intensity. In general, the higher the peak

Figure 11: Distribution of total storm activity for January.

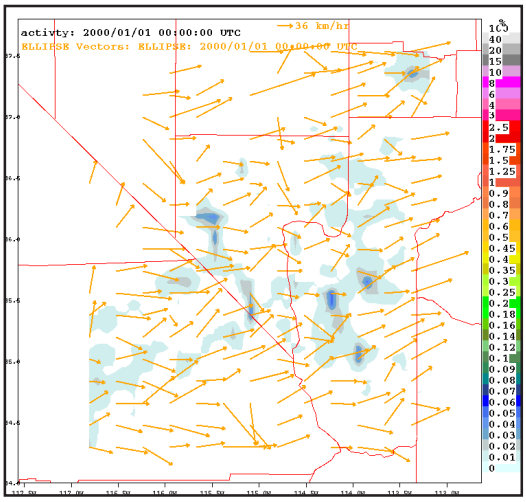

Figure 12: Distribution of total storm activity for February.

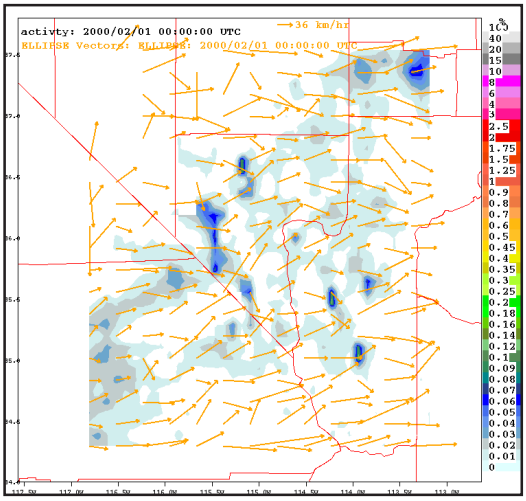

Figure 13: Distribution of total storm activity for March.

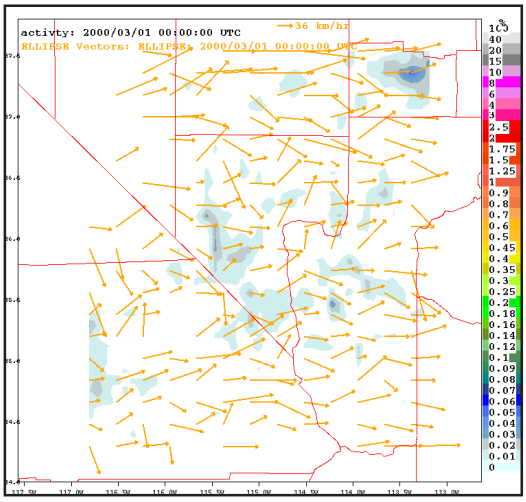

Figure 14: Distribution of total storm activity for April.

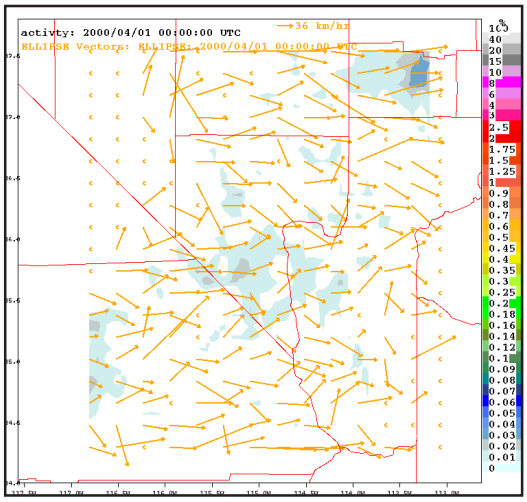

Figure 15: Distribution of total storm activity for May.

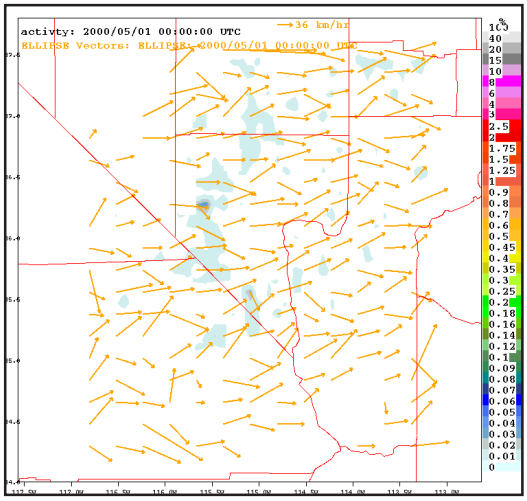

Figure 16: Distribution of total storm activity for June.

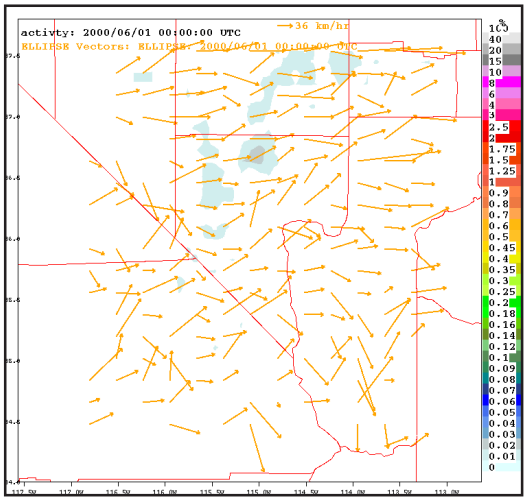

Figure 17: Distribution of total storm activity for July.

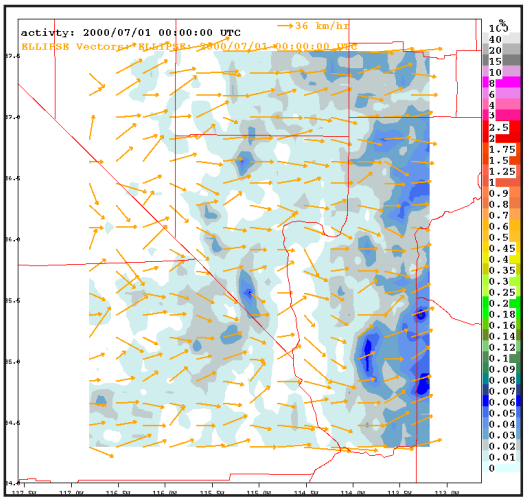

Figure 18: Distribution of total storm activity for August.

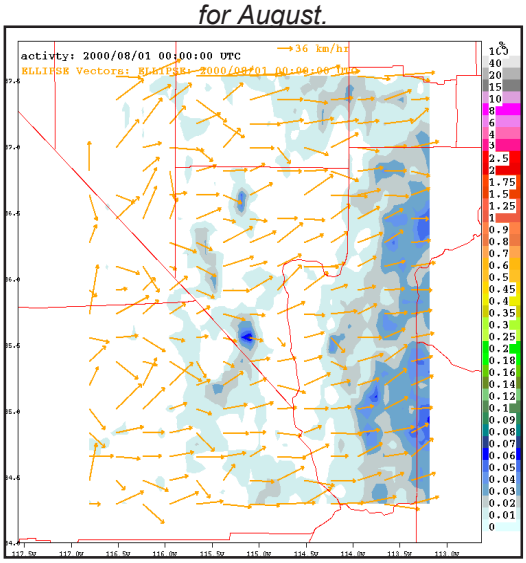

Figure 19: Distribution of total storm activity for September.

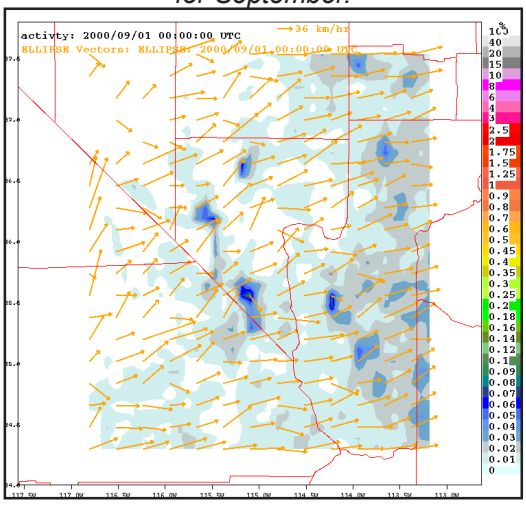

Figure 20: Distribution of total storm activity for October.

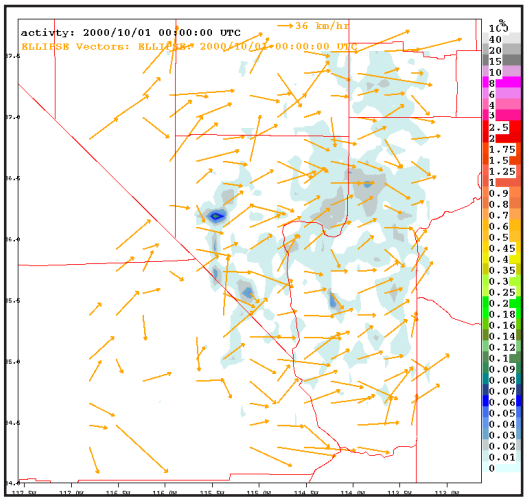

Figure 21: Distribution of total storm activity for November.

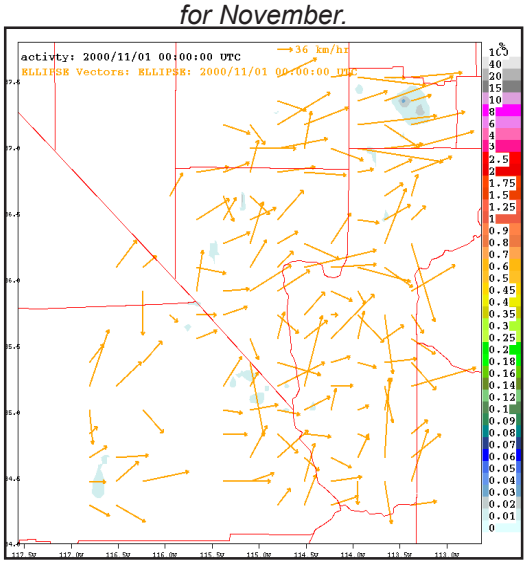

Figure 22: Distribution of total storm activity for November.

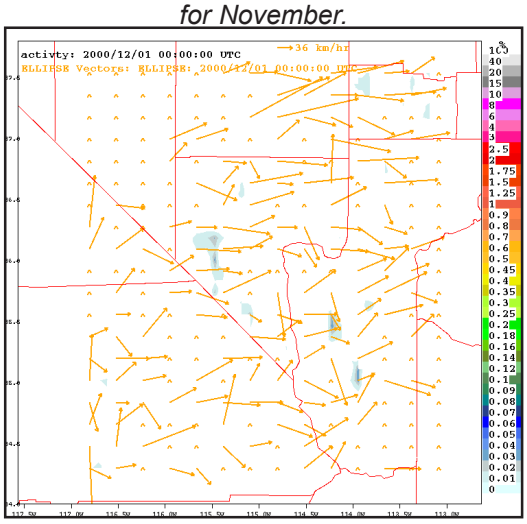

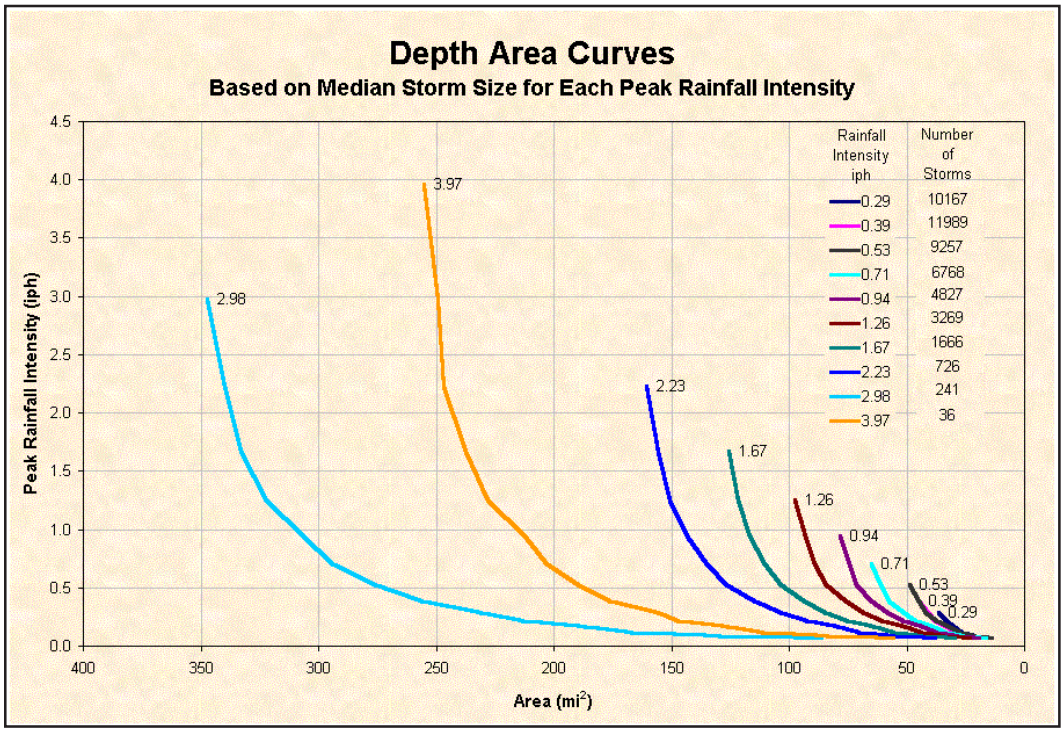

Figure 23: Depth area curves

Figure 24: Accumulated storm area curves

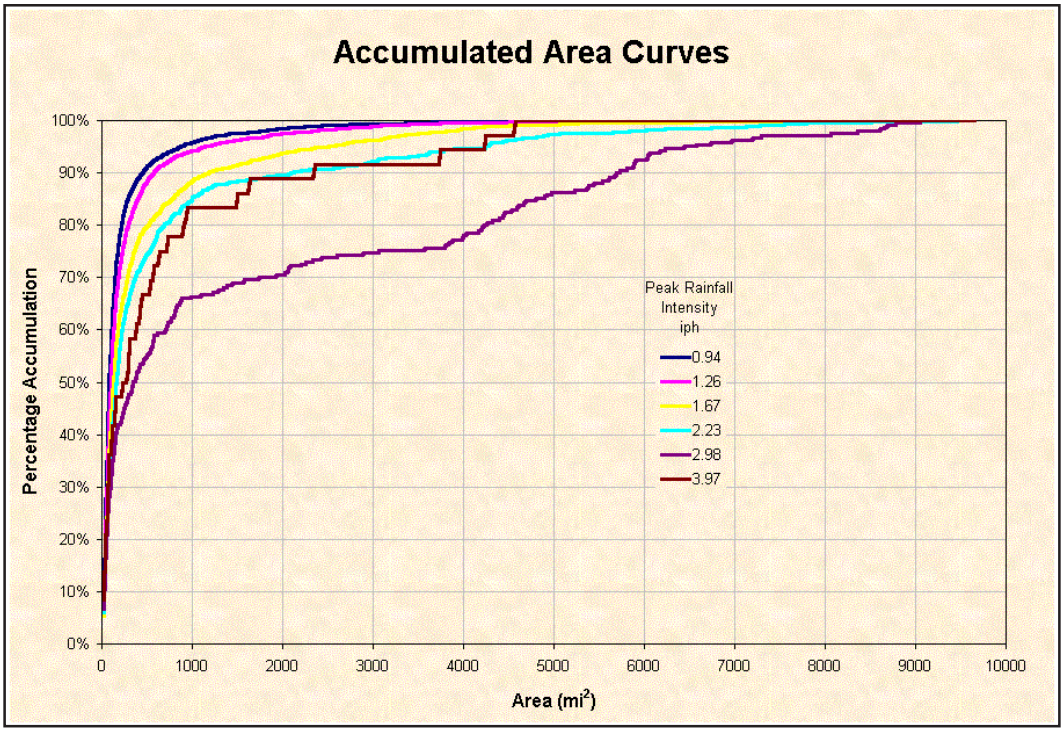

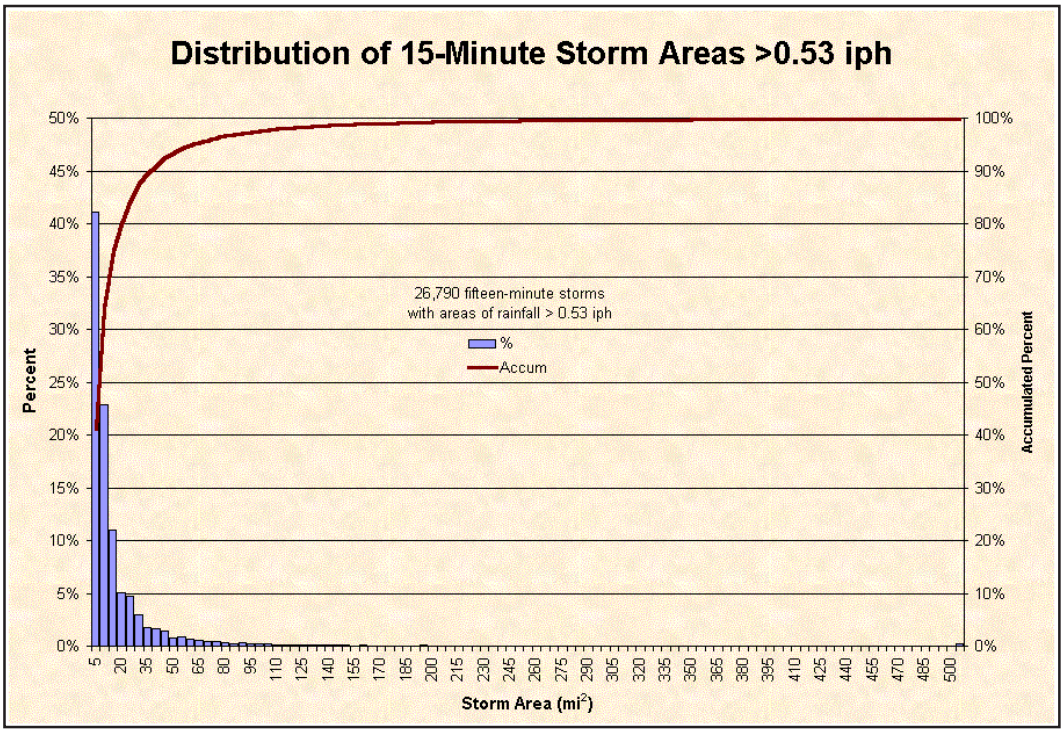

Figure 25: Distribution of 15-minute storm areas >0.53 iph

rainfall intensity, the larger the storm area. For example, the median size of storms with a peak intensity of 3.97 iph was 255 mi^2. Note the sharp horizontal gradients near each peak intensity. The depth-area curve for a storm with peak intensity of 3.97 iph shows that the portion of the storm with intensities between about 1.0 iph and 3.97 iph amounts to less than 12% of the total storm area, on average.

Of particular interest to rain gage network design is the expected size of the high intensity portions of storms and the network's ability to reliably detect them. Figure 25 shows the distribution of the portions of storms with rainfall rates equal to or exceeding 0.53 iph. Nearly 27,000 storms with rainfall intensities of 0.53 iph or greater were detected during the study period. The median of storm areas with intensities of 0.53 iph or greater was 6.77 mi^2. More than 90% of these areas were less than 100 square miles.

One possible anomaly in Figure 23 should be noted. The curves show an orderly increase in median storm area as peak rainfall intensity increases. The anomaly or exception is the curve for storms with peak intensities of 2.98 iph. This median storm size for the 2.98 iph storm was much larger than expected. It could just be a statistical anomaly due to the small number of storms in the top two categories, 2.98 iph and 3.97 iph. The number of storms in these two categories totals just 241 and 36 storms respectively or 0.2% of the total number of storms studied. It's also possible that there were some residual effects of ground clutter in this intensity range that affected the results.

Figure 24 presents another look at this problem. Figure 24 shows the area accumulation curves for the four curves with the highest rainfall intensities. The accumulation curve for storms with peak intensities of 2.98 iph is clearly different in shape than the other curves, which are all very similar to one another.

Summary

A historical database of 2 km x 2 km 15-minute radar-rainfall estimates was used to study the sizes, shapes, orientations, and depth-area characteristics of storms in Clark County, NV. More than 100,000 individual 15-minute storms were evaluated over a four year period. The size, shape, orientation, track, and the three-dimensional characteristics of each storm were cataloged.

Some of the most interesting findings of this study include the high number of storms available to evaluate from a radar-rainfall database, the small size of storms, and the even smaller size of the high intensity central intensities of storms. All of these findings have significant implications for hydrologic design.

For example, at the 15-minute level, storm areas with rainfall rates exceeding 0.5 iph were found to have a median size of 6.7 square miles. Compare this result to the average rain gage density of one gage per 65 square miles over Clark County. Only the highest density portions of Clark County's gage network in the Las Vegas approach the median size of these high intensity storm areas. The result is that the vast majority of high intensity events go undetected.

The small size found for high intensity events brings into question the practice of using spatially uniform rainfall at each time step for design storms. The results of this study suggest that storms in Clark County are very dynamic and higly variable. Assuming a spatially uniform rainfall pattern during the peak intensities of design storms may produce unrealitically high runoff computations.

The findings of this study and similar ones conducted in Florida and southern California offer a glimpse of the potential for large scale analysis of radar-rainfall estimates. The growing historical database of radar-rainfall offers an unprecidented opportunity to develop a more complete picture of the spatial distribution of rainfall.

References

Bradley, A. Allen, et. al., *Raingage Network Design Using NEXRAD Precipitation Estimates*, Submitted to **Journal of the American Water Resources Association**, 1999

Brakensiek, D.L., H.B. Osborn, and W.J. Rawls, coordinators*, Field Manual for Research on Agricultural Hydrology*, USDA, Agricultural Handbook, 1979

Bleasdale, A. *Rain Gauge Networks Development and Design with Special Reference to the United Kingdom*, in Proceedings of the WMO/IASH Symposium the Design of Hydrological Networks, IASH Pub. No. 67, pp 46-54, 1965

Curtis, David C., and Brett Clyde, *Comparing Spatial Distributions of Rainfall Derived from Rain Gages and Radar,* **Journal of Floodplain Management**, California Flood Plain Managers Association, July 1999

Dixon, Michael and Gerry Wiener, *TITAN: Thunderstorm Identification, Tracking, Analysis, and Nowcasting - A Radar-based Methodology*, Journal of Atmospheric and Oceanic Technology, Vol. 10, No. 6, December 1993

Dixon, Michael, **Automated Storm Identification, Tracking and Forecasting - A Radar-based Method**, Cooperative Thesis No. 148, University of Colorado and the National Center For Atmospheric Research, Boulder, CO, 1994

Grosch, R.C., *Relationships Between Severe Weather and Echo Tops in Central Illinois,* Preprints: 10th Conference on Severe Local Storms, American Meteorological Society, Boston, MA, 1977

Institute of Hydrology, *Methods for Evaluating the UK Rain Gauge Network*, 1977

Institute of Water Engineers, *Report of Joint Committee to Consider Methods of Determining General Rainfall Over Any Area*, Transactions of the Institute of Water Engineers, XLII, 231-259, 1937

Kelsch, M., *An Evaluation of the NEXRAD Hydrology Sequence for Different Types of Convective Storms in Northeastern Colorado*, Preprints: 24th Radar Meteorology Conference, American Meteorological Society, 1989

World Meteorological Organization, *Intercomparison of Conceptual Models Used in Operational Hydrologic Forecasting*, **Operational Hydrology Report No. 7, Annex III**, p 47, Geneva, Switzerland, 1975

World Meteorological Organization, **Guide to Hydrometeorological Practices**, Geneva, Switzerland, 1965

LEARN MORE

OneRain Incorporated
1531 Skyway Drive, Unit D
Longmont, Colorado 80504, USA

+1-303-774-2033
www.onerain.com